Pergamon

Int. J. Solids Structures Vol. 35, Nos 28–29, pp. 3635–3653, 1998

0020-7683/98 $19.00 + .00

PII: S0020-7683(97)00235-7

A HEAT TRANSFER ANALYSIS FOR QUARTZ MICRORESONATOR IR SENSORS

G. BAO* and W. JIANG
Department of Mechanical Engineering, The Johns Hopkins University, Baltimore, MD 21218, U.S.A.

(*Received* 17 *September* 1996; *in revised form* 25 *June* 1997)

Abstract—To aid the design of uncooled IR sensors based on quartz microresonators, a heat transfer analysis is carried out for the time-dependent temperature distribution in the resonator. The quartz resonator is taken to be circular, homogeneous isotropic, with a ring electrode on its front surface which is IR illuminated. It is assumed that the microresonator array is packaged in high vacuum; the side and back surfaces of the resonator are thermally insulated. Only heat conduction within the quartz resonator is considered; radiation at the surfaces and heat conduction through the bridges that link the resonator to the base structure are neglected. The boundary value problem of heat conduction in the resonator is solved analytically; expressions for the temperature distribution before and after the photon flux is turned off are given. It is found that for the quartz resonator under study, the time t_s required to reach a uniform temperature distribution in the entire resonator (the time constant) is critically dependent on the photon absorptivity of the ring electrode on the front surface. For example, when the ring electrode has no effect on photon absorption, $t_s = 9.52$ microseconds; however, if the ring electrode is fully reflective, $t_s = 4.76$ milliseconds. These time constants are expected to play an important role in the design of the quartz microresonator IR sensors.

1. INTRODUCTION

Requiring no visible light to "see" in the dark, infrared (IR) sensors enjoy a wide range of commercial and military applications. In general, IR sensors can be divided into two categories: photon detectors which are usually cooled, and thermal detectors which may not need to be cooled. Photon detectors are usually semiconductor devices with photoconductors, Schottky diodes, quantum well infrared photodetectors, or photovoltatic devices as the sensing elements, while in the thermal detectors the sensing elements include thermocouples, bolometers, Golay cells, and pyroelectric devices (Kruse *et al.*, 1963; Schlessinger, 1995). Recently, a microresonator-based high-sensitivity sensor and sensor array is proposed by Vig *et al.* (1996) for use as uncooled IR sensors. This new class of IR sensors has the potential to surpass the performance of other types of IR sensors, be they photon detectors or thermal detectors. The design and fabrication of microresonator-based IR sensors, however, pose many challenging problems.

Microresonators may have thickness $h = 1$–10 μm and diameter $D = 100$–1000 μm, with resonance frequencies of the fundamental mode (thickness shear mode) in the range of 100–1000 MHz. Although such microresonators are not suitable for precision frequency control applications due to their extremely high sensitivity to mass loading, they can be used for IR detection and imaging, and for chemical and biological agent sensing. In particular, when quartz is used as the resonator material, the temperature dependence of the resonance frequency can be utilized to make precision thermometers (Gorini and Sartori, 1962; Wade and Slutsky, 1962; Smith and Spencer, 1963; Ziegler and Tiesmeyer, 1983; Hamrour and Galliou, 1994). It is possible to sense temperature changes of microkelvins, since quartz resonators' frequency can vary with temperature monotonically with a slope of about 10^{-4}/°K (Vig *et al.*, 1996). With a proper resonator cut, the temperature sensitivity of the sensor can be maximized (Heising, 1946). It is this temperature dependence of the resonance frequency that enables one to develop microresonator IR sensors (Vig *et al.*, 1996).

* Author to whom correspondence should be addressed.

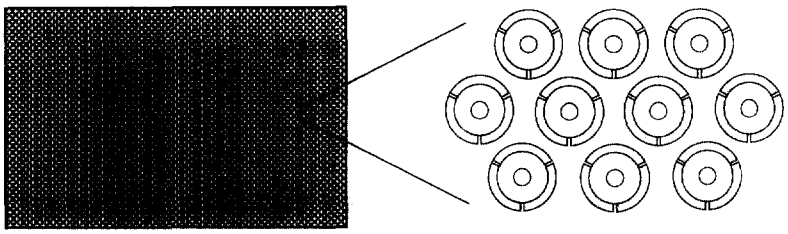

Fig. 1. A schematic of an IR sensor array consisting of circular microresonators.

As shown schematically in Fig. 1, the IR sensor array consists of a large number of microresonators. For example, within an area of 6.4×9 cm, about 80,000, 600 MHz quartz resonators can be produced (Vig *et al.*, 1996). Upon absorbing photons emitted from an IR source, each individual resonator has a temperature increase ΔT, which in turn causes a shift in the resonance frequency Δf. Converting the measured frequency changes to a color code on a gray scale, a video image of the IR emitting body can be generated. Clearly, the quality of the image depends on the number of resonators per unit area, and the temperature coefficient of frequency. For an IR sensor array, its performance is determined by many other parameters including the IR absorbance, the thermal conductance to a heat sink, and the time constant (the time required to reach a uniform temperature) (Vig *et al.*, 1996). Successful design of an IR sensor array requires a detailed analysis of the influences of each of these parameters.

Although quartz itself is a good IR absorbing material near 9, 12, 20 and 26 μm wavelengths (Spitzer and Kleiman, 1961), a thin metal coating may be deposited to the front (the IR illuminated) surface of the resonator to absorb photons more effectively from the IR source. To further increase the absorption, an IR reflecting film may be deposited on the entire back side of the resonator so that the IR energy transmitted through the quartz plate is reflected back. Since these coatings are usually very thin (~ 10 nm), their effects on the resonance frequency of the quartz plate can be neglected.

A quartz resonator usually has its major surfaces covered by electrodes made of a thin sheet of metal such as aluminum. Since an electrode made of aluminum reflects most of the IR energy, in order to maximize the IR absorption, the quartz microresonator IR sensors are designed to have a ring electrode on the IR illuminated surface (Steward and Kim, 1996; Vig *et al.*, 1996). Even with an IR absorbing coating, the ring electrode usually has a lower photon absorptivity than the rest of the front surface of the resonator, resulting in a non-uniform absorption of the incident IR energy, and leading to a time-dependent, non-uniform temperature distribution in the resonator before and long after the photon flux is turned off. Consequently, the shift in the resonance frequency changes within a certain period of time. Since the resonance frequency-temperature relationship of a quartz resonator is calibrated assuming a uniform temperature field (Mason, 1950; Salt, 1987), it is necessary to calculate the time needed to reach the uniform temperature field in the resonator (the time constant) in order to determine the timing of IR image measurement. The aim of this paper is to examine the transient thermal behavior of the resonator due to the presence of the ring electrode on the front surface, and to predict the time constant.

The rest of the paper is organized as follows. The configuration of the resonator and the basic assumptions made in the analysis is discussed in Section 2. In Section 3, the boundary value problem of the heat equation is solved. Predictions of the temperature distributions in and the time constant of the resonator are given in Section 4. The conclusions and discussions of the model assumptions are presented in Section 5.

2. PRELIMINARIES

Consider a single quartz resonator in the IR sensor array, as shown schematically in Fig. 2(a). The intensity of the IR source is assumed to be uniform across the front surface

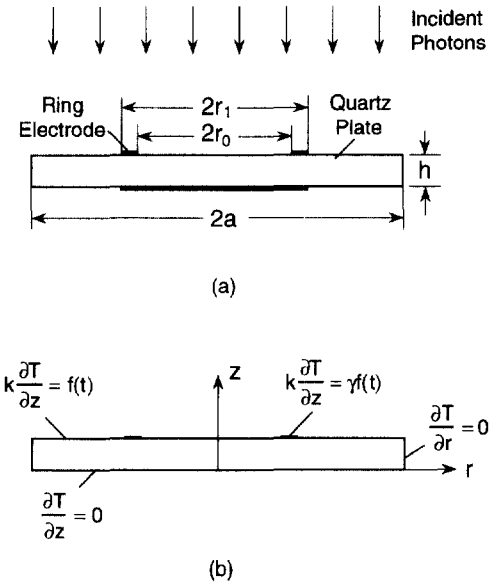

Fig. 2. The heat transfer problem of a circular quartz resonator shown in (a) with a ring electrode on the IR illuminated surface can be formulated with the boundary conditions given in (b). The dimensions of the resonator and the ring electrode are also shown.

of a single resonator, but varies from resonator to resonator. The resonator is assumed to be a circular rotated Y-cut (e.g., AC-cut) quartz plate with thickness h and radius a, coated with a thin metal film on the front surface, and linked to the base-structure (a heat sink) by three evenly spaced narrow bridges in order to achieve a controlled amount of thermal isolation (Fig. 1). A ring electrode (made, e.g., aluminum) with inner radius r_0 and outer radius r_1, and a circular electrode plate with radius r_1 are, respectively, vacuum deposited to the front and back surfaces of the quartz resonator. The ring electrode (possibly with a photon-absorbing coating) on the front surface is assumed to absorb a fraction of the incident IR energy. The effect of multiple reflections of the incident IR energy within the resonator due to the existence of the electrode (and possibly an IR reflecting film) on the back surface is neglected.

As mentioned earlier, the front surface ($z = h$) of the quartz resonator absorbs photons emitted from the IR source. The resulting heat flux along the negative z-direction can be estimated by (Kruse *et al.*, 1963)

$$q = \beta N hc/\lambda \tag{1}$$

where β is the fraction of absorbed energy (absorptivity), N is the number of photons per second input per unit area, $h = 6.6252 \times 10^{-34}$ W s^2 is Planck's constant, c is the speed of light, and λ is the wavelength. The underlying assumption in eqn (1) is that the front surface of the resonator is coated with a porous photon-absorptive thin (~ 10 nm) metal film so that most of the incident IR energy is absorbed by this thin film (Lang *et al.*, 1992). Consequently, the dependence of photon absorption on the thickness of the resonator can be neglected, and the heat flux induced by the incident IR energy can be taken as a surface source.

Generally speaking, the value of β in eqn (1) depends on the material of the resonator, and the wavelength. Without coating, a 2.5 μm thick quartz plate in the 8–14 μm IR band has $\beta = 0.17$ (Palik, 1985). With an IR absorbing coating, the value of β can be much higher. For example, at a critical thickness of 12 nm and wavelength of 10 μm, a vacuum evaporated gold film has $\beta \approx 0.5$ (Lang *et al.*, 1992). A porous silver film under similar conditions can have $\beta > 0.99$ (Lang *et al.*, 1992). To make the present study more generic, in what follows, the heat flux q is taken as a design parameter without specifying explicitly the value of β.

The heat transfer problem of the quartz microresonator shown in Fig. 1 is in general very complex, since heat conduction, convection and radiation can all be present. However, when the IR sensor array is packaged in high vacuum, heat convection can be neglected, and heat conduction from the resonator to the surrounding media is only through the bridges. The thermal conductance G of the resonator due to both conduction via quartz bridges and radiation from the surface of the resonator can be estimated by (Vig *et al.*, 1996)

$$G = \frac{knwb}{L} + 8\pi\sigma T^3 a^2 \tag{2}$$

where $k(=8.3$ W/mK) is the effective isotropic thermal conductivity of quartz, n, w, b and L are the number, width, thickness, and length of the bridges, a and T are the radius and temperature of the resonator, and $\sigma = 5.67 \times 10^{-8}$ W/m^2 K^4 is the Stefan–Boltzmann constant. To simplify the heat transfer analysis, in the following, we assume that $G = 0$, i.e., we neglect heat conduction due to the bridges, and radiation. (This assumption will be discussed in more detail in Section 5.) Thus, as indicated in Fig. 2(b), at the cylindrical surface ($r = a$) and the back surface ($z = 0$) of the resonator, the heat flux is zero, i.e.,

$$\frac{\partial T}{\partial z} = 0, \quad z = 0, \quad 0 \leqslant r \leqslant a \tag{3a}$$

$$\frac{\partial T}{\partial r} = 0, \quad r = a, \quad 0 \leqslant z < h. \tag{3b}$$

For an IR sensor with cut-off time t_c (the time at which the photon flux is turned off; usually t_c is a fraction of the frame time), the time-dependent incident heat flux $f(t)$ at the front surface can be given by

$$\begin{aligned} f(t) &= q, \quad 0 < t < t_c \\ &= 0, \quad t > t_c. \end{aligned} \tag{4}$$

Since the resonator is in high vacuum, it is assumed that the non-zero heat flux at $z = h$ is entirely due to photon absorption. The boundary condition at $z = h$ is thus given by (Fig. 2(b))

$$\begin{aligned} k\left.\frac{\partial T}{\partial z}\right|_{z=h} &= f(t), \quad 0 \leqslant r < r_0 \\ &= \gamma f(t), \quad r_0 < r < r_1 \\ &= f(t), \quad r_1 < r \leqslant a \end{aligned} \tag{5}$$

where γ is the relative absorptivity of the ring electrode. If the ring electrode has no effect on photon absorption ("fully" absorptive), $\gamma = 1$; if it is fully reflective, $\gamma = 0$. Note that according to (1), the ring electrode has absorptivity $\gamma\beta$.

In summary, the boundary value problem of heat conduction in the circular quartz resonator consists of the following governing equation and initial and boundary conditions:

$$\frac{\partial T}{\partial t} = \alpha \nabla^2 T \tag{6a}$$

$$T|_{t=0} = T_0 \tag{6b}$$

$$\left.\frac{\partial T}{\partial r}\right|_{r=a} = 0 \tag{6c}$$

$$\left.\frac{\partial T}{\partial z}\right|_{z=0} = 0 \tag{6d}$$

$$\left.\frac{\partial T}{\partial z}\right|_{z=h} = \eta(r,t) \tag{6e}$$

where T_0 is a reference temperature, $\alpha = k/\rho c_p$ is the thermal diffusivity, with ρ and c_p being the density and specific heat of quartz, respectively;

$$\begin{aligned}\eta(r,t) &= f(t)/k, \quad 0 \leqslant r < r_0 \\ &= \gamma f(t)/k, \quad r_0 < r < r_1 \\ &= f(t)/k, \quad r_1 < r \leqslant a\end{aligned} \tag{7}$$

and $T(r,z,t)$ in (6) is the temperature field in the resonator. Although the thermal conductivity of quartz is orthotropic, for simplicity, in this study, the quartz resonator is taken to be isotropic. Further, the thickness increase due to the electrodes is neglected. Let

$$T(r,z,t) = u(r,z,t) + T_0; \tag{8}$$

the boundary value problem defined in (6) becomes

$$\frac{\partial u}{\partial t} = \alpha\left[\frac{1}{r}\frac{\partial}{\partial r}\left(r\frac{\partial u}{\partial r}\right) + \frac{\partial^2 u}{\partial z^2}\right] \tag{9a}$$

$$u|_{t=0} = 0 \tag{9b}$$

$$\left.\frac{\partial u}{\partial r}\right|_{r=a} = 0 \tag{9c}$$

$$\left.\frac{\partial u}{\partial z}\right|_{z=0} = 0 \tag{9d}$$

$$\left.\frac{\partial u}{\partial z}\right|_{z=h} = \eta(r,t). \tag{9e}$$

The solution of the governing equation (9a), together with the initial and boundary conditions given in (9b)–(9e), is discussed in the next section.

3. SOLUTIONS OF HEAT CONDUCTION

The heat conduction problem defined in eqn (9) and (7) is solved by performing Laplace transform (Arpaci, 1966)

$$\hat{u}(r,z,p) = \int_0^\infty u(r,z,t)\, e^{-pt}\, \mathrm{d}t \tag{10}$$

to eqn (9a) and the boundary conditions (9b)–(9e). Using the initial condition (9b), we have

$$\nabla^2 \hat{u} - \frac{p}{\alpha}\hat{u} = 0 \tag{11a}$$

with

$$\left.\frac{\partial \hat{u}}{\partial r}\right|_{r=a} = 0 \tag{11b}$$

$$\left.\frac{\partial \hat{u}}{\partial z}\right|_{z=0} = 0 \tag{11c}$$

$$\left.\frac{\partial \hat{u}}{\partial z}\right|_{z=h} = F(r,p) \tag{11d}$$

where $F(r,p)$ is Laplace transform of $\eta(r,t)$:

$$\begin{aligned} F(r,p) &= \frac{q}{kp}(1-e^{-pt_c}), \quad 0 \leqslant r < r_0 \\ &= \frac{\gamma q}{kp}(1-e^{-pt_c}), \quad r_0 < r < r_1 \\ &= \frac{q}{kp}(1-e^{-pt_c}), \quad r_1 < r \leqslant a. \end{aligned} \tag{12}$$

Solving Helmholtz eqn (11a), together with the homogeneous boundary conditions (11b) and (11c) using the separation of variables approach, we have

$$\hat{u}(r,z,p) = \sum_{i=0}^{\infty} A_i J_0(k_i r)\cosh \omega_i z \tag{13}$$

where

$$\omega_i = \sqrt{k_i^2 + p/\alpha}; \tag{14a}$$

$J_0(x)$ is the Bessel function of order zero, k_i are the eigenvalues given by

$$k_i = \mu_i/a \tag{14b}$$

with μ_i being the roots of

$$J_1(\mu_i) = 0 \tag{14c}$$

where $J_1(x)$ is the Bessel function of order one. For convenience, we assume that $\mu_0 < \mu_1 < \mu_2 < \mu_3 < \cdots$. Note that $\mu_0 = 0$, i.e., $k_0 = 0$. The unknown constants A_i are obtained by satisfying the boundary condition (11d):

$$A_0 = \frac{q(1-e^{-pt_c})}{kp\omega_0 \sinh \omega_0 h}\left[1 + (1-\gamma)\left(\frac{r_0^2}{a^2} - \frac{r_1^2}{a^2}\right)\right] \tag{15a}$$

$$A_i = \frac{2q(1-e^{-pt_c})(1-\gamma)}{kpak_i\omega_i J_0(k_i a)\sinh \omega_i h}\left[\frac{r_0}{a}\frac{J_1(k_i r_0)}{J_0(k_i a)} - \frac{r_1}{a}\frac{J_1(k_i r_1)}{J_0(k_i a)}\right], \quad i = 1,2,3,\ldots \tag{15b}$$

Performing the inversion of Laplace transform to $\hat{u}(r,z,p)$ given in eqn (13), we have for the temperature field $u(r,z,t)$ in the resonator (Appendix A):

(i) for $0 < t \leqslant t_c$,

$$u(r,z,t)=\frac{qh}{k}\left[1+(1-\gamma)\left(\frac{r_0^2}{a^2}-\frac{r_1^2}{a^2}\right)\right]\left[\frac{\alpha t}{h^2}+\frac{1}{2}\left(\frac{z^2}{h^2}-\frac{1}{3}\right)\right.$$
$$\left.-\frac{2}{h^2}\sum_{n=1}^{\infty}\frac{(-1)^n}{\lambda_n^2}e^{-\alpha\lambda_n^2 t}\cos\lambda_n z\right]+\frac{2q(1-\gamma)}{kha}\sum_{i=1}^{\infty}\frac{1}{k_i}\frac{J_0(k_i r)}{J_0(k_i a)}\left[\frac{r_0}{a}\frac{J_1(k_i r_0)}{J_0(k_i a)}-\frac{r_1}{a}\frac{J_1(k_i r_1)}{J_0(k_i a)}\right]$$
$$\times\left[\frac{1}{k_i^2}(1-e^{-\alpha k_i^2 t})+2\sum_{n=1}^{\infty}\frac{(-1)^n}{k_i^2+\lambda_n^2}(1-e^{-\alpha(k_i^2+\lambda_n^2)t})\cos\lambda_n z\right]; \quad (16a)$$

(ii) for $t \geqslant t_c$,

$$u(r,z,t)=\frac{qh}{k}\left[1+(1-\gamma)\left(\frac{r_0^2}{a^2}-\frac{r_1^2}{a^2}\right)\right]$$
$$\times\left[\frac{\alpha t_c}{h^2}+\frac{2}{h^2}\sum_{n=1}^{\infty}\frac{(-1)^n}{\lambda_n^2}(e^{-\alpha\lambda_n^2(t-t_c)}-e^{-\alpha\lambda_n^2 t})\cos\lambda_n z\right]$$
$$+\frac{2q(1-\gamma)}{kha}\sum_{i=1}^{\infty}\frac{1}{k_i}\frac{J_0(k_i r)}{J_0(k_i a)}\left[\frac{r_0}{a}\frac{J_1(k_i r_0)}{J_0(k_i a)}-\frac{r_1}{a}\frac{J_1(k_i r_1)}{J_0(k_i a)}\right]$$
$$\times\left[\frac{1}{k_i^2}(e^{-\alpha k_i^2(t-t_c)}-e^{-\alpha k_i^2 t})+2\sum_{n=1}^{\infty}\frac{(-1)^n}{k_i^2+\lambda_n^2}\right.$$
$$\left.\times(e^{-\alpha(k_i^2+\lambda_n^2)(t-t_c)}-e^{-\alpha(k_i^2+\lambda_n^2)t})\cos\lambda_n z\right] \quad (16b)$$

where

$$\lambda_n=\frac{n\pi}{h} \quad n=1,2,3,\ldots \quad (17)$$

Solutions of the heat transfer problem for several special designs of the resonator can be obtained directly from (16). First, if the photons from the IR source is focused onto the circular area inside the ring electrode for energy-trapping purposes (Steward and Kim, 1996), the temperature field is obtained readily from (16) by setting $r_1 = a$, $\gamma = 0$. Second, when the effect of the ring electrode on photon absorption can be neglected, i.e., $\gamma = 1$, the temperature field in the resonator, which is identical to that in an infinitely large quartz plate $u(z,t)$ (Appendix B), can be obtained from (16) by letting $r_0 = r_1$, or $\gamma = 1$:

(i) for $0 < t \leqslant t_c$,

$$u(z,t)=\frac{qh}{k}\left[\frac{\alpha t}{h^2}+\frac{1}{2}\left(\frac{z^2}{h^2}-\frac{1}{3}\right)-\frac{2}{h^2}\sum_{n=1}^{\infty}\frac{(-1)^n}{\lambda_n^2}e^{-\alpha\lambda_n^2 t}\cos\lambda_n z\right]; \quad (18a)$$

(ii) for $t \geqslant t_c$,

$$u(z,t)=\frac{qh}{k}\left[\frac{\alpha t_c}{h^2}+\frac{2}{h^2}\sum_{n=1}^{\infty}\frac{(-1)^n}{\lambda_n^2}(e^{-\alpha\lambda_n^2(t-t_c)}-e^{-\alpha\lambda_n^2 t})\cos\lambda_n z\right]. \quad (18b)$$

Note that h^2/α (α is the thermal diffusivity of quartz) has the dimension of time and can be used as a characteristic time scale.

4. TEMPERATURE DISTRIBUTION IN THE RESONATOR

A unique feature in the design of quartz microresonator IR sensors is the presence of a ring electrode on the front surface which can be fully absorptive, partially absorptive, or fully reflective. To gain insight, in the following, these three types of ring electrodes are modeled, and their effects on heat transfer in the resonator quantified. Emphasis is placed on the prediction of the time constants of the resonator. For all the cases considered in this section, the resonator and the ring electrode are assumed to have dimensions $a/h = 30$, $r_0/a = 1/6$, $r_1/a = 1/3$. Since the electrode is very thin and has a high thermal diffusivity compared with the quartz plate, the time required to diffuse heat into the ring electrode is neglected.

4.1. *Fully absorptive ring electrode*, $\gamma = 1$

When the effect of the ring electrode on photon absorption at the front surface is negligible, $\gamma = 1$. In this case the temperature field in the resonator is given by eqn (18) which is independent of the radial position r in the resonator. As illustrated in Fig. 3, when time t is such that $0.2h^2/\alpha < t \leqslant t_c$, temperature in the resonator increases linearly with time t. However, when $t > t_c$, temperature in the resonator approaches rapidly to a constant value. In Fig. 3, the normalized temperature $(T-T_0)k/qh$ is plotted against the nondimensional time $\alpha t/h^2$ for $z/h = 0.2, 0.4, 0.6, 0.8, 1.0$ for $\alpha t_c/h^2 = 3.0$. Note that after the photon flux is turned off at $t = t_c$, it takes only $t_s = t - t_c \approx 0.4h^2/\alpha$ to reach the steady-state uniform temperature $T = T_0 + \alpha q t_c/kh$. For a quartz resonator with $\alpha = 4.2 \times 10^{-6}$ m^2/s (Mills, 1992) and $h = 10$ μm, t_s is merely 9.5 microseconds. To further illustrate this feature, in Fig. 4, the relative temperature $(T-T_0)k/qh - \alpha q t_c/kh$ is displayed as a function of $\alpha(t-t_c)/h^2$ for $z/h = 0.2, 0.4, 0.6, 0.8$ and 1.0. It is worth mentioning that the time constant $t_s = 0.4h^2/\alpha$ is found to be independent of the cut-off time t_c.

The time constant t_s determines when the IR image measurement should be taken after the photon flux is turned off at $t = t_c$; it plays an important role in the design of quartz

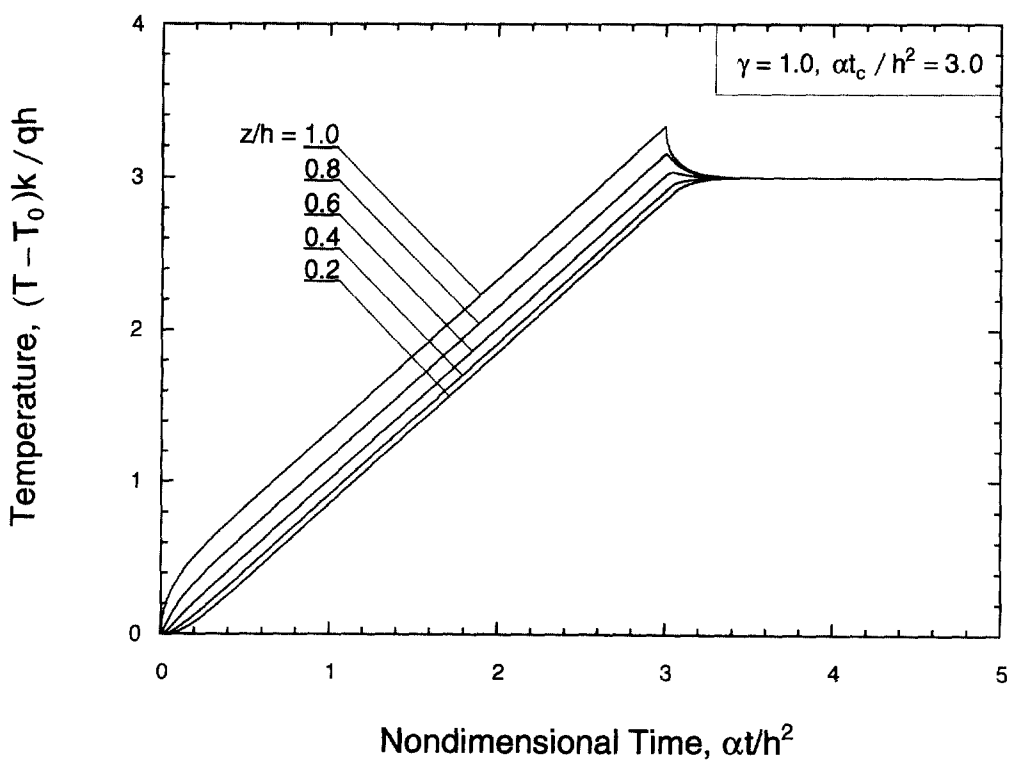

Fig. 3. Normalized temperature $(T-T_0)k/qh$ as a function of the nondimensional time $\alpha t/h^2$ at $z/h = 0.2, 0.4, 0.6, 0.8, 1.0$ for a resonator with a fully absorptive ring electrode ($\gamma = 1$). The cut-off time is taken to be $\alpha t_c/h^2 = 3.0$.

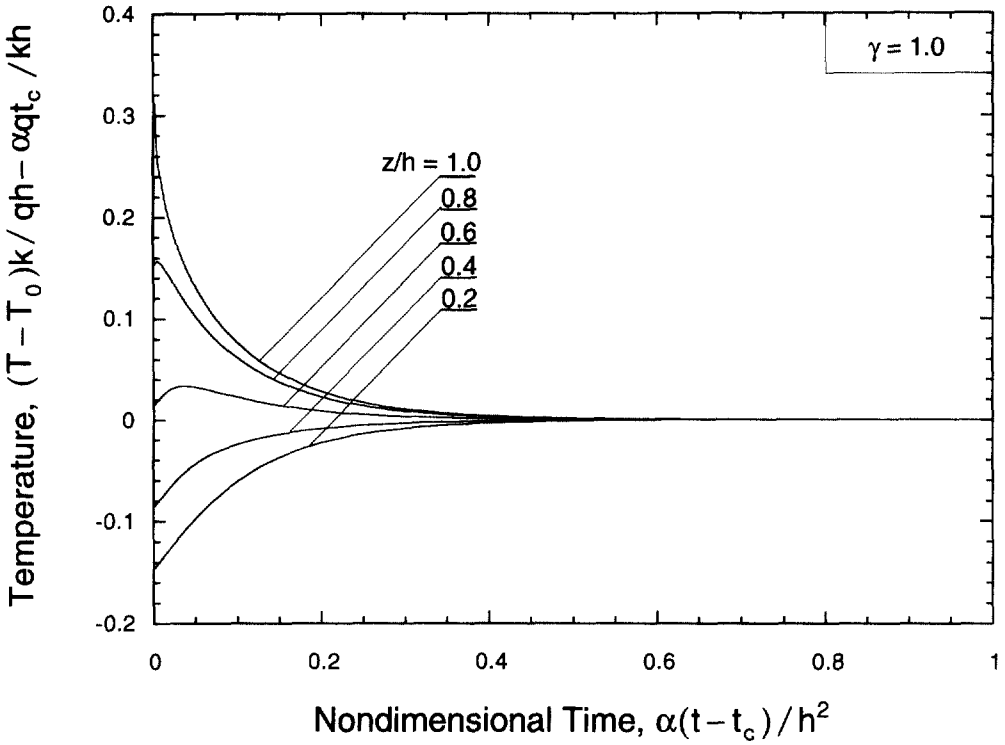

Fig. 4. The temperature distribution after the photon flux is turned off as shown by the normalized temperature $(T-T_0)k/qh-\alpha qt_c/h$ as a function of the nondimensional time $\alpha(t-t_c)/h^2$ at $z/h = 0.2$, 0.4, 0.6, 0.8, 1.0 for a resonator with $\gamma = 1$. The curves shown are independent of the cut-off time t_c.

microresonator IR sensors. Usually the relationship between the change in temperature ΔT and change in resonance frequency Δf is calibrated assuming that temperature in the resonator is uniform. Thus, if the IR image is taken before time t reaches t_c+t_s, the nonuniform temperature distribution in the resonator may render the calibrated relationship between ΔT and Δf invalid. For a resonator with a fully absorptive ring electrode, the very small time constant implies that temperature in the resonator becomes uniform shortly after the photon flux is turned off, and the IR images can be taken with a short frame time. However, in reality, the ring electrode may be partially absorptive or even fully reflective, and the corresponding time constant t_s may become large, as will be discussed in the following sub-sections.

4.2. *Fully reflective ring electrode*, $\gamma = 0$

When the ring electrode has no photon absorption, $\gamma = 0$, i.e., the incident heat flux is zero for $r_0 < r < r_1$; the resulting temperature distribution in the resonator is highly nonuniform. Shown in Fig. 5(a) is the normalized temperature $(T-T_0)k/qh$ as a function of the radial position r/a at $\alpha t/h^2 = 1.0$ for $z/h = 0.2$, 0.4, 0.6, 0.8 and 1.0. The temperature distribution for the resonator with $\gamma = 1$ is also shown for comparison. It is seen that temperature increases with z, as might be expected. It is clear that there is a shape drop in temperature in the region beneath the ring-electrode. Due to the high temperature gradient near the edges of the ring electrode, heat flows into the region underneath the ring-electrode from other regions. To drive this point home, in Fig. 5(b), $(T-T_0)k/qh$ is plotted as a function of r/a at a larger time scale $\alpha t/h^2 = 10.0$. The curves in Fig. 5(b) demonstrate that due to heat conduction, temperature in the region beneath the ring is increased compared with that at $\alpha t/h^2 = 1$. This implies that, compared with the case of a fully absorptive ring electrode, it will take a much longer time to reach a uniform temperature distribution in the resonator.

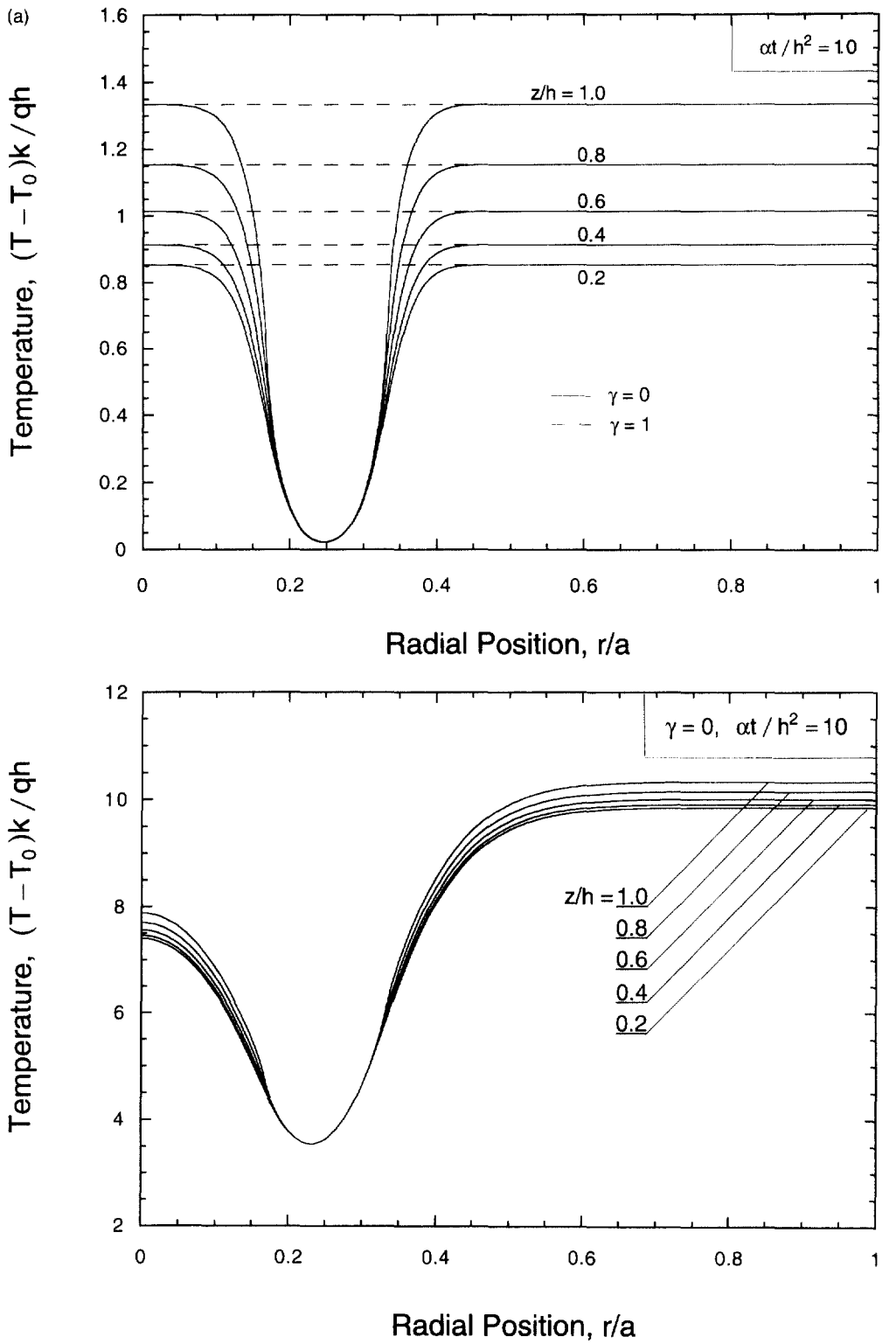

Fig. 5. Normalized temperature $(T-T_0)k/qh$ as a function of the radial position r/a at $z/h = 0.2$, 0.4, 0.6, 0.8, 1.0 at (a) $\alpha t/h^2 = 1.0$ and (b) $\alpha t/h^2 = 10.0$ for a resonator with a fully reflective ring electrode ($\gamma = 0$) with $a/h = 30$, $r_0/a = 1/6$, $r_1/a = 1/3$. The temperature distribution for a resonator with $\gamma = 1$ is also shown in (a) for comparison.

To show how the temperature distribution in an IR microresonator becomes uniform after the photon flux is turned off, in Fig. 6(a), curves of $(T-T_0)k/qh$ vs r/a are shown for $\alpha t/h^2 = 4$, 8, 12, 20, 50, 100 and 200. The cut-off time is taken to be $\alpha t_c/h^2 = 3$. For a microresonator with $a/h = 30$, $r_0/a = 1/6$, $r_1/a = 1/3$, it takes $\alpha(t-t_c)/h^2 \approx 200$ to reach a rather uniform temperature distribution. This implies that for the quartz resonator with $h = 10$ μm, $t_s \approx 4.76$ ms. This time constant t_s is found to be independent of the cut-off time t_c, as can be seen from Fig. 6(b) in which the curves of $(T-T_0)k/qh$ as a function of r/a are plotted for $\alpha t_c/h^2 = 300$ (for a quartz resonator with $h = 10$ μm and cut-off time $t_c = 10$ ms, $\alpha t_c/h^2 = 385$). Note that in Fig. 6(a) and (b), temperature in the resonator is calculated after it becomes uniform in the thickness direction.

4.3. *Partially absorptive ring electrode*, $0 < \gamma < 1$

The ring electrode on the front surface may have partial absorption of the incident photons, i.e., $0 < \gamma < 1$. To quantify the influence of photon absorption of the ring electrode, calculations were carried out for the temperature distribution in the quartz resonator at nondimensional time $\alpha t/h^2 = 1.0$, 10.0 and 100.0. Shown in Fig. 7(a) are curves of the normalized temperature $(T-T_0)k/qh$ vs radial position r/a in the resonator for $\alpha t/h^2 = 1.0$, $z/h = 0.5$ for $\gamma = 0.0$, 0.2, 0.4, 0.6, 0.8 and 1.0. Note that $\gamma = 0$ and $\gamma = 1$ correspond to fully reflective and fully absorptive ring electrodes, respectively. Evidently, for a ring electrode with a small value of γ, the drop in temperature in the region beneath the ring-electrode is significant. The high temperature gradient near the edges of the ring electrode causes heat to flow into the region covered by the ring-electrode. The non-uniformity of the temperature distribution decreases as γ increases, as can be seen from Fig. 7(a). Though less dramatic, the same general trends are true at larger time scales, as illustrated in Fig. 7(b) and (c) in which curves of $(T-T_0)k/qh$ vs r/a are shown for $\alpha t/h^2 = 10.0$ and 100.0, respectively. For all the curves shown in Fig. 7(a)–(c), it is assumed that $t < t_c$.

As mentioned earlier, a small t_s is desirable in designing the quartz resonator IR sensors. To reduce the time constant t_s, one can increase the relative absorptivity γ of the ring electrode by using a more absorptive metal for the electrode, or by depositing a photon-absorbing coating on the electrode. To illustrate the effect of γ on the time constant t_s, in Fig. 8, t_s is shown as a function of γ for the quartz resonator under consideration ($a/h = 30$, $r_0/a = 1/6$, $r_1/a = 1/3$) for cut-off time $\alpha t_c/h^2 = 300$. In calculating t_s, the maximum value of the relative variation in the temperature $(T-T_0)k/qh$ along the radial direction for $0 \leqslant r \leqslant a$ is set to be 0.005. It is seen from Fig. 8 that, for $0 < \gamma < 0.8$, t_s decreases with γ rather slowly. For example, at $\gamma = 0.8$, $\alpha t_s/h^2 = 94$, which is about half of the value at $\gamma = 0$. To significantly reduce the time constant t_s, the fraction γ of photon absorption of the ring electrode has to be larger than 0.8. Note that the design curve shown in Fig. 8 is valid for other values of t_c as well since the time constant t_s is essentially independent of the cut-off time t_c. However, it depends on the dimensions of the resonator as well as the ring electrode.

5. CONCLUDING DISCUSSIONS

To aid the design of uncooled IR sensors based on quartz microresonators, a heat transfer analysis is carried out for the time-dependent temperature distribution in the quartz resonator which has a ring electrode on the IR illuminated surface. Emphasis is placed on the effect of the ring electrode on the transient thermal behavior of the resonator; the effect of the electrodes on the dispersion relations of the resonator can be found in Steward and Kim (1996). The ring electrode is assumed to have a relative photon absorptivity $0 \leqslant \gamma \leqslant 1$ while the region outside the ring electrode always has $\gamma = 1$. Only heat conduction within the quartz resonator is considered; radiation at the surfaces and heat conduction through the bridges that link the resonator to the base structure are neglected. The boundary value problem of heat conduction in the resonator is solved analytically; expressions for the transient temperature distribution before and after the photon flux is turned off are given.

The solution of the temperature field in the resonator indicates that after the photon flux is turned off at $t = t_c$, it takes only $t_s \approx 0.4h^2/\alpha$ to reach a uniform temperature distribution in the thickness direction. When the ring electrode has no effect on the photon

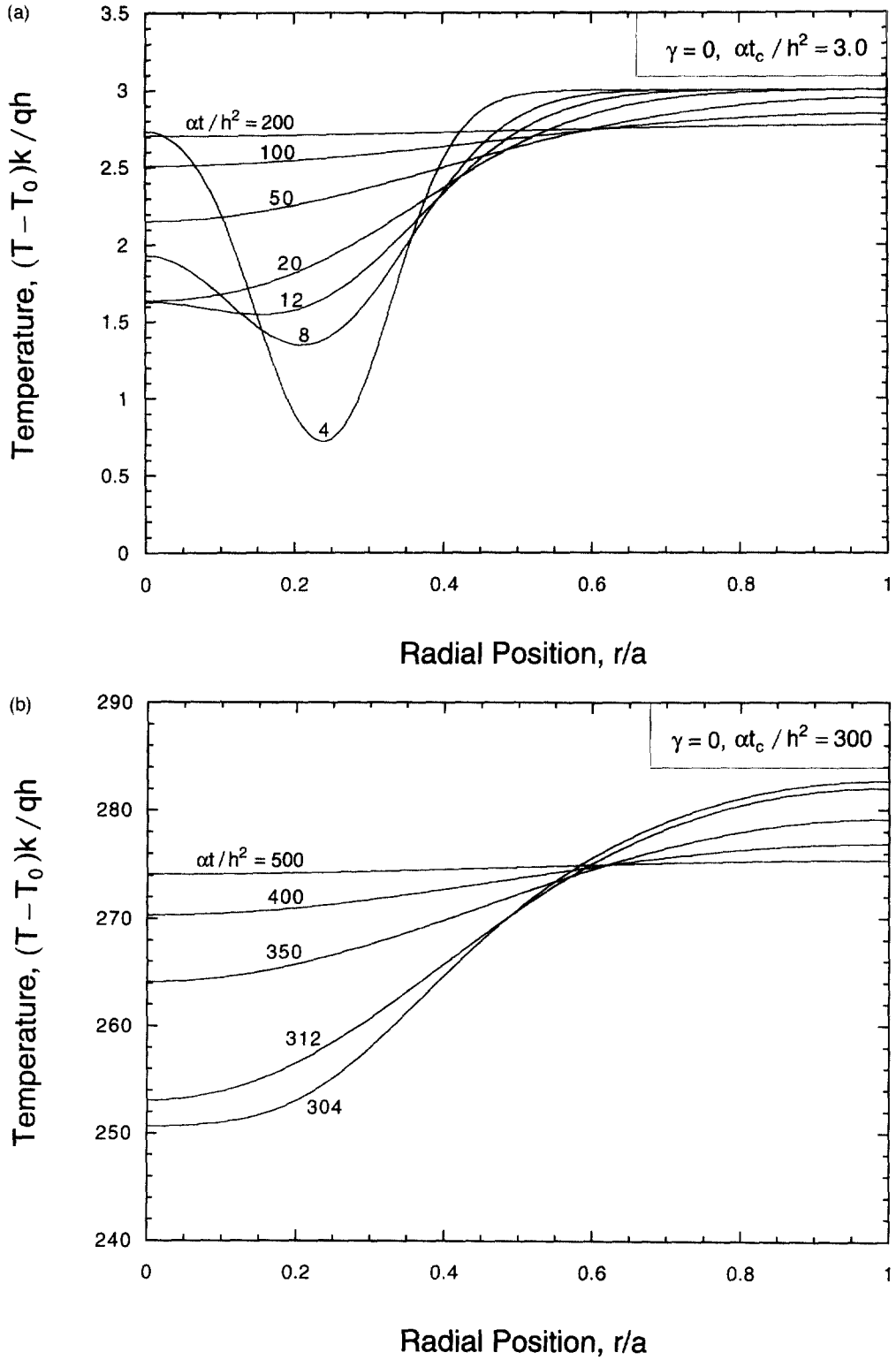

Fig. 6. The temperature distribution in the resonator becomes uniform as time t increases after the photon flux is turned off. Shown are $(T-T_0)k/qh$ vs r/a curves at different nondimensional time $\alpha t/h^2$. The cut-off time is taken to be $\alpha t_c/h^2 = 3.0$ in (a) and $\alpha t_c/h^2 = 300.0$ in (b). Note that the time needed to reach the steady state is a constant $t_s \approx 200h^2/\alpha$ independent of the cut-off time t_c.

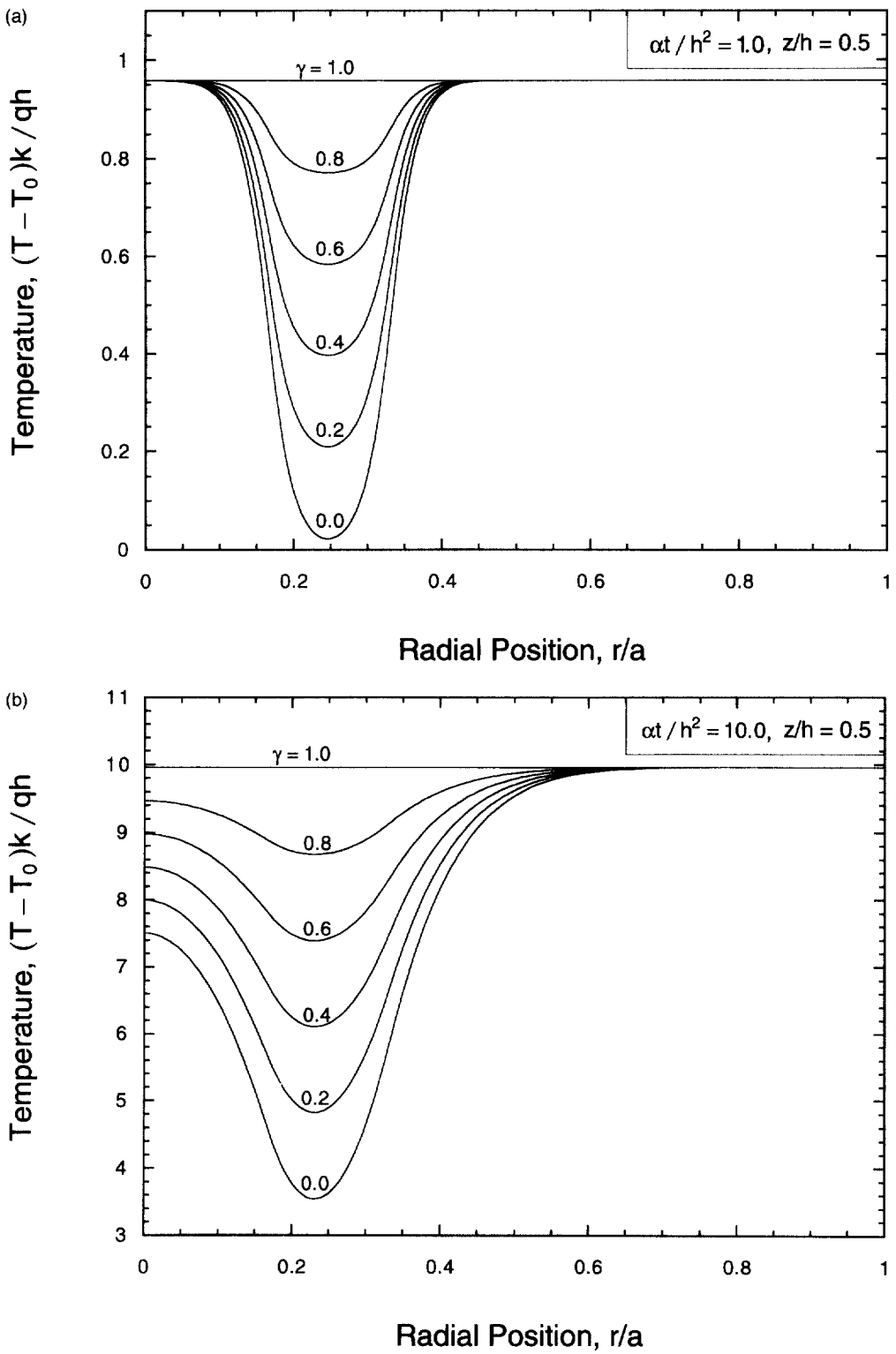

Fig. 7. The normalized temperature $(T-T_0)k/qh$ vs radial position r/a for $z/h = 0.5$, $\gamma = 0.0$, 0.2, 0.4, 0.6, 0.8 and 1.0 for (a) $\alpha t/h^2 = 1.0$, (b) $\alpha t/h^2 = 10.0$, and (c) $\alpha t/h^2 = 100.0$.

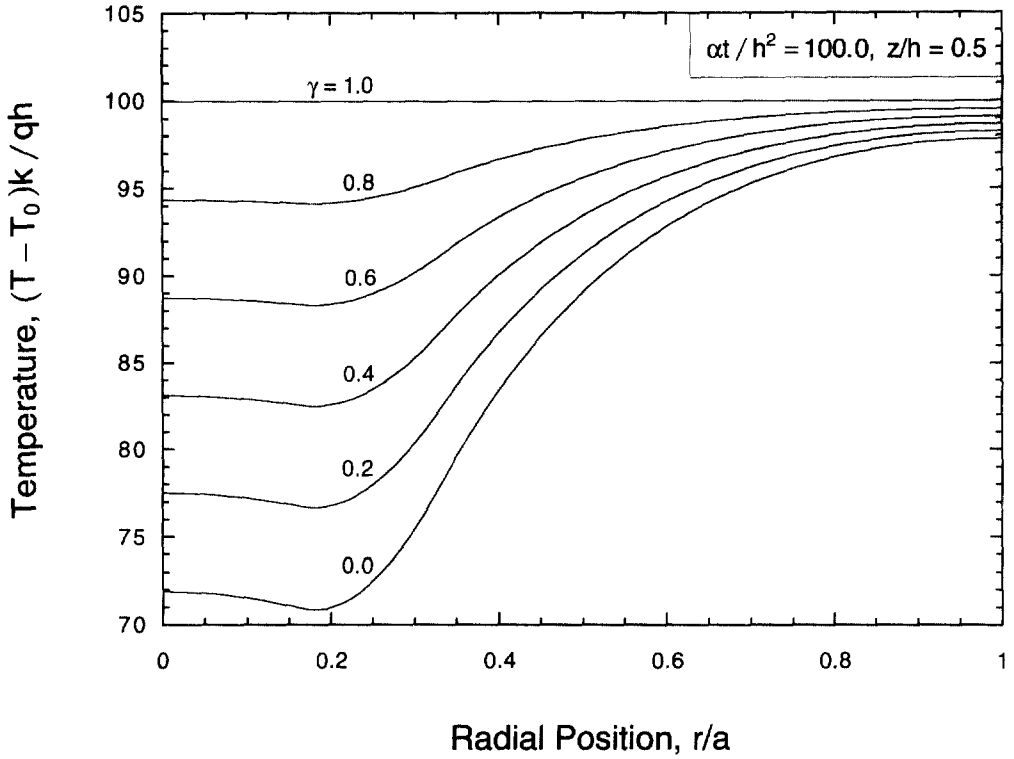

Fig. 7.—*Continued.*

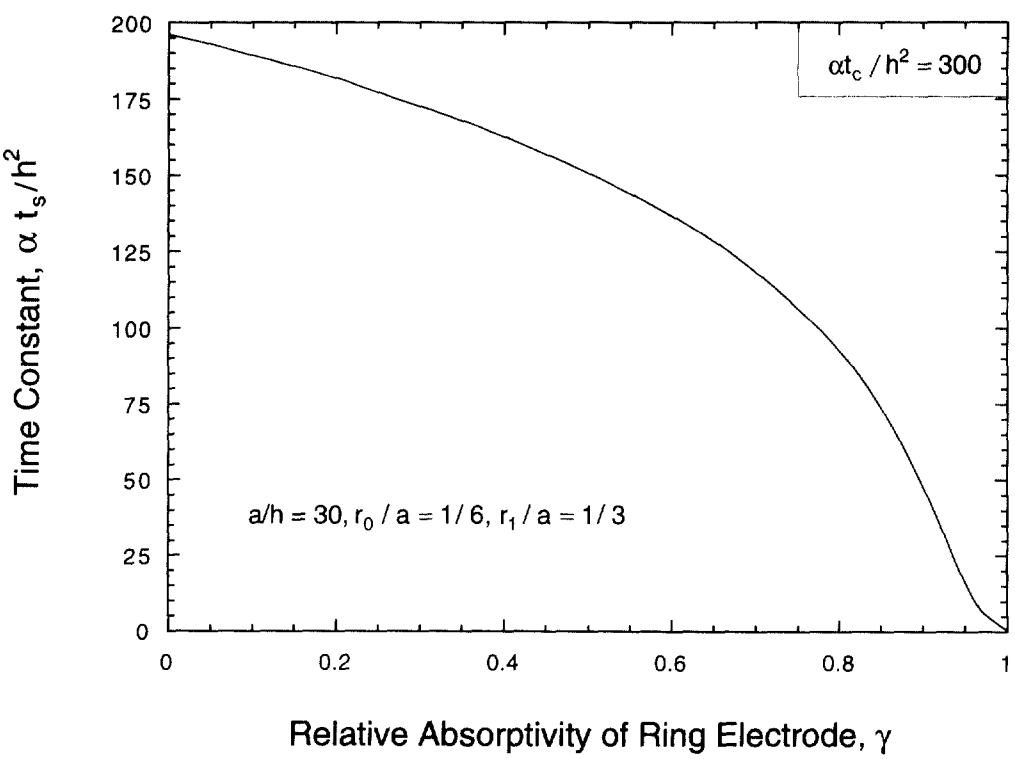

Fig. 8. The time constant t_s as a function of the relative absorptivity γ for the quartz resonator under consideration ($a/h = 30$, $r_0/a = 1/6$, $r_1/a = 1/3$) for cut-off time $\alpha t_c/h^2 = 300$.

absorption (i.e., $\gamma = 1$), this is the time required to have a constant temperature in the entire resonator (the time constant). For example, for a quartz resonator with thickness $h = 10$ μm, $t_s = 9.5$ μs. However, when a fully-reflective ring electrode (i.e., $\gamma = 0$) with $r_0/a = 1/6$, $r_1/a = 1/3$ is placed on the front surface of the resonator, it takes $t_s \approx 200h^2/\alpha$ to reach a uniform temperature distribution in the entire resonator. For a quartz resonator with thickness $h = 10$ μm, the corresponding time constant $t_s = 4.76$ ms. When the ring electrode is photon-absorptive with absorptivity γ, the time constant t_s is a function of γ. It is found that the time constant t_s can be significantly reduced only if $\gamma \geqslant 0.8$.

The very large difference (500-fold) in the time constants t_s can be understood as follows. When the ring electrode is fully absorptive, in order to reach a uniform temperature in the resonator, the heat flux at the front surface only needs to travel through a distance h (the thickness). For a quartz resonator with thickness $h = 10$ μm and thermal diffusivity $\alpha = 4.2 \times 10^{-6}$ m^2/s, the corresponding characteristic time scale for thermal diffusion is given by $t_1 = h^2/\alpha = 23.8$ microseconds. On the other hand, when the ring electrode is fully reflective, heat flux needs to travel a distance about $0.7a$ (with a being the radius of the resonator) to realize a uniform temperature distribution, as can be seen from Fig. 5(a). This corresponds to a characteristic time scale $t_2 = (0.7a)^2/\alpha = 10.5$ milliseconds if $a/h = 30$ is assumed. The ratio of these two characteristic time scales t_2/t_1 is 441 which is quite similar to the 500-fold difference in the time constants. Clearly, the geometry and size of the quartz plate and the ring electrode can have a significant effect on the values of the time constant t_s; such an effect should be further quantified.

The time constant t_s plays an important role in the design of the quartz microresonator IR sensor array, since it determines when the IR image measurement should be taken after the photon flux is turned off at $t = t_c$. Usually the relationship between the change in temperature ΔT and change in resonance frequency Δf is calibrated assuming that temperature in the resonator is uniform. Thus, if the IR image is taken before time t reaches $t_c + t_s$, the nonuniform temperature distribution in the resonator may render the calibrated relationship between ΔT and Δf invalid. One way to reduce the time constant t_s is to increase the relative absorptivity γ of the ring electrode by using a more absorptive metal for the electrode, or depositing a photon absorbing coating on the electrode. However, as indicated by the curve shown in Fig. 8, in order to significantly reduce the time constant t_s, the electrode material or the coating should be selected such that $\gamma \geqslant 0.8$.

To simplify the thermal analysis for the quartz microresonator IR sensors, in this study, several assumptions are made. For example, the thermal conductivity k of quartz is taken to be isotropic, although in reality it is orthotropic. For example, at 300°K, the thermal conductivity along the optical axis direction is $k_1 = 10.4$ W/mK, while perpendicular to the optical axis it is $k_2 = 6.2$ W/mK. Since the values of the thermal conductivity in the radial and thickness directions of a rotated Y-cut quartz plate are within the range $k_2 \leqslant k \leqslant k_1$, in the isotropic approximation, we simply take $k = (k_1 + k_2)/2$. This approximation gives a relative error of less than 26% of the predicted time constants. Although desirable, an analytical solution of the heat transfer problem of a circular quartz plate is difficult to obtain when the orthotropy of thermal conductivity is included, since the corresponding problem is no longer axisymmetric. When the microresonator is made of a rectangular Y-cut quartz plate, an analytic solution of the heat transfer problem including the material anisotropy is given in Bao (1997).

In the heat transfer analysis given above, the relatively small effect of multiple reflections of incident IR energy in the quartz plate is neglected. A simple calculation using optical multi-reflection theory indicates that a 10 μm thick quartz plate with a gold mirror attached to the back of the resonator will have about 10% higher absorption than that without the mirror (Kim, 1996). Further, when the front surface of the resonator is coated with a thin ($\sim$ 10 nm) porous photon-absorptive metal film, most of the incident IR energy is absorbed by this thin film (Lang *et al.*, 1992). It is therefore reasonable to assume that the photon absorption does not depend on the thickness of the resonator, and the resulting heat flux acts as a surface source, as indicated by eqn (1). A detailed numerical quantification is needed in future studies of the effect of multiple reflections in the quartz resonator without a thin IR absorbing film on the front surface.

As mentioned earlier, a real IR microresonator has heat conduction through the bridges and radiation at the resonator surface. The effects of the bridges and radiation on the transient behavior are neglected in this study (i.e., $G = 0$) since they are secondary compared with that of the ring electrode. Specifically, for the microresonator IR sensors considered in this study, the thermal conductance G is

$$G = \frac{knwb}{L} + 8\pi\sigma T^3 a^2 = 53.26 \times 10^{-6} \text{W/K} \tag{20}$$

where $k = 8.3$ W/mK, $n = 3$, $w = b = 10$ μm, $L = 50$ μm, $a = 300$ μm. $T = 300$°K are assumed. The corresponding thermal time constant of the resonator is given by (Kruse *et al.*, 1963)

$$\tau_T = \frac{c_v \pi a^2 h}{G} = 104.8 \text{ milliseconds} \tag{21}$$

where $c_v = 1.974 \times 10^6$ Ws/m^3 K is the specific heat of quartz. Since τ_T is much larger compared with the long time constant $t_s = 4.76$ milliseconds for the resonator with a fully reflective ring electrode, the effect of assuming $G = 0$ is very small. Needless to say, the above analysis is just an estimate, the exact influence of heat conduction via the bridges on the time constant t_s should be quantified (using, e.g., a finite element analysis). It is also necessary to analyze thermal conduction in quartz resonators of rectangular geometry (Bao, 1997), since they have a higher fill factor than the circular ones.

Acknowledgements—This work was supported by the Army Research Laboratory, Physical Sciences Division under the Microelectronics Research Collaborative Program. Special thanks go to Drs John R. Vig and Yoonkee Kim at ARL/PSD.

REFERENCES

Arpaci, V. S. (1966) *Conduction Heat Transfer*. Addison-Wesley, London.
Bao, G. (1997) Heat conduction in rectangular quartz microresonator IR sensors, to be published.
Gorini, I. and Sartori, S. (1962) Quartz thermometer. *Rev. Sci. Instr.* **33,** 883–884.
Gradshteyn, I. S. and Ryzhik, I. M. (1980) *Table of Integrals, Series, and Products*. Academic Press, London.
Hamrour, M. R. and Galliou, S. (1994) Analysis of the infrared sensitivity of a quartz resonator application as a thermal sensor. *Proc. Ultrasonics Symp.*, pp. 362–364.
Heising, R. A. (1946) *Quartz Crystals for Electrical Circuits*. Van Nostrand Reinhold, New York.
Kim, Y. (1996) Private communication.
Kruse, P. W., McGlauchlin, L. D. and McQuistan, R. B. (1962) *Elements of Infrared Technology*. John Wiley and Sons, New York.
Lang, W., Kühl, K. and Sandmaier, H. (1992) Absorbing layers for thermal infrared detectors. *Sensors and Actuators A* **34,** 243–248.
Mason, W. P. (1950) *Piezoelectric Crystals and Their Application to Ultrasonics*. Van Nostrand Reinhold, New York.
Mills, A. F. (1992) *Heat Transfer*. Irwin, Inc., Boston.
Morse, P. M. and Feshbach, H. (1953) *Methods of Theoretical Physics*. McGraw-Hill, New York.
Palik, E. D. (1985) *Handbook of Optical Constants of Solids*, Vol. 1. Academic Press, Orlando, FL.
Salt, D. (1987) *Hy-Q Handbook of Quartz Crystal Devices*. Nostrand Reinhold, New York.
Schlessinger, M. (1995) *Infrared Technology Fundamentals*. Marcel Dekker, New York.
Smith, W. L. and Spencer, W. J. (1963) Quartz crystal thermometer for measuring temperature derivations in the 10^{-3}–10^{-6}°C range. *Rev. Sci. Instr.* **34,** 268–270.
Spitzer, W. G. and Kleiman, D. A. (1961) Infrared lattice bands of quartz. *Physical Review* **121,** 1324–1335.
Steward, J. T. and Kim, Y. (1996) Design of a quartz microresonator for infrared sensor applications. Proceedings of the 1996 IEEE International Frequency Control Symposium, to be published.
Vig, J. R., Filler, R. L. and Kim, Y. (1996) Uncooled IR imaging array based on quartz resonators. *Journal of Microelectromechanical Systems* **5,** 131–137.
Wade, W. H. and Slutsky, L. J. (1962) Quartz crystal thermometer. *Rev. Sci. Instr.* **33,** 212–213.
Ziegler, H. and Tiesmeyer, J. (1983) Digital sensor for IR radiation. *Sensors and Actuators* **4,** 363–367.

APPENDIX A

From eqns (12) and (13), we have

$$\bar{u}(r,z,p)=\frac{q(1-e^{-pt_c})}{kp}\left[\frac{1}{\omega_0\sinh\omega_0 h}\left(1+(1-\gamma)\left(\frac{r_0^2}{a^2}-\frac{r_1^2}{a^2}\right)\right)\cosh\omega_0 h\right.$$
$$\left.+(1-\gamma)\sum_{i=1}^{\infty}\frac{2\cosh\omega_i z}{ak_i\omega_i\sinh\omega_i h}\frac{J_0(k_i r)}{J_0(k_i a)}\left(\frac{r_0}{a}\frac{J_1(k_i r_0)}{J_0(k_i a)}-\frac{r_1}{a}\frac{J_1(k_i r_1)}{J_0(k_i a)}\right)\right] \quad \text{(A1)}$$

where

$$\omega_0=\sqrt{p/\alpha},\quad \omega_i=\sqrt{k_i^2+p/\alpha}. \quad \text{(A2)}$$

Let

$$F_1(p)=\frac{q}{kp}(1-e^{-pt_c}) \quad \text{(A3)}$$

$$F_2(z,p)=\frac{1}{\omega_i}\frac{\cosh\omega_i z}{\sinh\omega_i h}. \quad \text{(A4)}$$

It is readily shown that the inversion of $kF_1(p)$ is the function $f(t)$ defined in (4). The inversion of $F_2(z,p)$, $g(z,t)$, can be obtained using the inversion theorem of Laplace transform

$$g(z,t)=\frac{1}{2\pi i}\int_L F_2(z,p)\,e^{pt}\,\mathrm{d}p \quad \text{(A5)}$$

where L is a straight line parallel to the imaginary axis in the complex p-plane; L is so chosen that in the region on the right side of L, $F_2(z,p)$ has no singularity. Defining a new integration variable s,

$$s=k_i^2+p/\alpha: \quad \text{(A6)}$$

eqn (A5) can be rewritten as

$$g(z,t)=\frac{\alpha}{2\pi i}\int_{\gamma-i\infty}^{\gamma+i\infty}\frac{\cosh\sqrt{s}z}{\sqrt{s}\sinh\sqrt{s}h}e^{\alpha(s-k_i^2)t}\,\mathrm{d}s. \quad \text{(A7)}$$

Note that although $\sqrt{s}$ is a multi-valued function of s, the integrand is single-valued. Note also that $\sinh\sqrt{sh}$ has infinitely many first-order poles s_n on the negative real axis

$$s_n=-\frac{n^2\pi^2}{h^2},\quad n=0,1,2,3,\ldots \quad \text{(A8)}$$

The integral in (A7) can be evaluated using the residual theorem (Morse and Feshbach, 1953)

$$g(z,t)=\alpha e^{-\alpha k_i^2 t}\sum_{n=0}^{\infty}\mathrm{Re}\,s\left[\frac{\cosh\sqrt{s}z}{\sqrt{s}\sinh\sqrt{s}h}e^{\alpha st},s_n\right]$$
$$=\frac{\alpha}{h}e^{-\alpha k_i^2 t}\left[1+2\sum_{n=1}^{\infty}(-1)^n e^{-\alpha\lambda_n^2 t}\cos\lambda_n z\right] \quad \text{(A9)}$$

where

$$\lambda_n=n\pi/h,\quad n=1,2,3,\ldots \quad \text{(A10)}$$

Applying the convolution integral of Laplace transform, we have

$$u(r,z,t)=\left[1+(1-\gamma)\left(\frac{r_0^2}{a^2}-\frac{r_1^2}{a^2}\right)\right]\frac{\alpha}{kh}\int_0^t f(\tau)\left[1+2\sum_{n=1}^{\infty}(-1)^n e^{-\alpha\lambda_n^2(t-\tau)}\cos\lambda_n z\right]\mathrm{d}\tau$$
$$+\frac{2\alpha(1-\gamma)}{akh}\sum_{i=1}^{\infty}\frac{1}{k_i}\frac{J_0(k_i r)}{J_0(k_i a)}\left[\frac{r_0}{a}\frac{J_1(k_i r_0)}{J_0(k_i a)}-\frac{r_1}{a}\frac{J_1(k_i r_1)}{J_0(k_i a)}\right]\times\int_0^t f(\tau)\,e^{-\alpha k_i^2(t-\tau)}\left[1+2\sum_{n=1}^{\infty}(-1)^n e^{-\alpha\lambda_n^2(t-\tau)}\cos\lambda_n z\right]\mathrm{d}\tau. \quad \text{(A11)}$$

Performing the integration with $f(t)$ defined in (4), the temperature field in the resonator is given by

(i) for $0<t\leqslant t_c$,

$$u(r,z,t)=\frac{qh}{k}\left[1+(1-\gamma)\left(\frac{r_0^2}{a^2}-\frac{r_1^2}{a^2}\right)\right]\left[\frac{\alpha t}{h^2}+\frac{1}{2}\left(\frac{z^2}{h^2}-\frac{1}{3}\right)-\frac{2}{h^2}\sum_{n=1}^{\infty}\frac{(-1)^n}{\lambda_n^2}e^{-\alpha\lambda_n^2 t}\cos\lambda_n z\right]$$

$$+\frac{2q(1-\gamma)}{kha}\sum_{i=1}^{\infty}\frac{1}{k_i}\frac{J_0(k_i r)}{J_0(k_i a)}\left[\frac{r_0}{a}\frac{J_1(k_i r_0)}{J_0(k_i a)}-\frac{r_1}{a}\frac{J_1(k_i r_1)}{J_0(k_i a)}\right]\times\left[\frac{1}{k_i^2}(1-e^{-\alpha k_i^2 t})+2\sum_{n=1}^{\infty}\frac{(-1)^n}{k_i^2+\lambda_n^2}(1-e^{-\alpha(k_i^2+\lambda_n^2)t})\cos\lambda_n z\right];$$

(ii) for $t \geqslant t_c$,

$$u(r,z,t)=\frac{qh}{k}\left[1+(1-\gamma)\left(\frac{r_0^2}{a^2}-\frac{r_1^2}{a^2}\right)\right]\left[\frac{\alpha t_c}{h^2}+\frac{2}{h^2}\sum_{n=1}^{\infty}\frac{(-1)^n}{\lambda_n^2}(e^{-\alpha\lambda_n^2(t-t_c)}-e^{-\alpha\lambda_n^2 t})\cos\lambda_n z\right]$$

$$+\frac{2q(1-\gamma)}{kha}\sum_{i=1}^{\infty}\frac{1}{k_i}\frac{J_0(k_i r)}{J_0(k_i a)}\left[\frac{r_0}{a}\frac{J_1(k_i r_0)}{J_0(k_i a)}-\frac{r_1}{a}\frac{J_1(k_i r_1)}{J_0(k_i a)}\right]$$

$$\times\left[\frac{1}{k_i^2}(e^{-\alpha k_i^2(t-t_c)}-e^{-\alpha k_i^2 t})+2\sum_{n=1}^{\infty}\frac{(-1)^n}{k_i^2+\lambda_n^2}(e^{-\alpha(k_i^2+\lambda_n^2)(t-t_c)}-e^{-\alpha(k_i^2+\lambda_n^2)t})\cos\lambda_n z\right]. \tag{16b}$$

APPENDIX B

Consider heat conduction of an infinitely large quartz plate with thickness h. At the front surface $z=h$, due to the heat flux generated by IR illumination, we have

$$k\frac{\partial T}{\partial z}\bigg|_{z=h}=f(t) \tag{B1}$$

where $T(z,t)$ is the temperature field and $f(t)$ is defined in (4). At the back surface $z=0$, $\partial T/\partial z=0$. Assuming that $u(z,t)=T(z,t)-T_0$, the boundary value problem for $u(z,t)$ is given by

$$\frac{\partial u}{\partial t}=\alpha\frac{\partial^2 u}{\partial z^2} \tag{B2}$$

$$u|_{t=0}=0 \tag{B3}$$

$$\frac{\partial u}{\partial z}\bigg|_{z=0}=0 \tag{B4}$$

$$\frac{\partial u}{\partial z}\bigg|_{z=h}=f(t)/k \tag{B5}$$

where α is the thermal diffusivity of quartz.

Let

$$\hat{u}(\lambda_n,t)=\sqrt{\frac{2}{h}}\int_0^h u(z,t)\cos\lambda_n z\,\mathrm{d}z \tag{B6}$$

where $\lambda_n=n\pi/h$. Applying the Fourier transform (B6) to the governing equation (B2), performing integration by parts, and using the boundary conditions, we have

$$\frac{\mathrm{d}\hat{u}}{\mathrm{d}t}+\alpha\lambda_n^2\hat{u}=(-1)^n\frac{\alpha}{k}\sqrt{\frac{2}{h}}f(t). \tag{B7}$$

Solving (B7) with the initial condition (B3) yields

(i) $n=0$,

$$u(z,t)=\frac{\alpha}{k}\sqrt{\frac{2}{h}}\int_0^t f(\tau)\,\mathrm{d}\tau; \tag{B8}$$

(ii) $n\neq 0$, $n=1,2,3,\ldots$,

$$u(z,t)=\frac{2\alpha}{kh}\sum_{n=1}^{\infty}(-1)^n e^{-\alpha\lambda_n^2 t}\cos\lambda_n z\int_0^t f(\tau)\,e^{\alpha\lambda_n^2\tau}\,\mathrm{d}\tau. \tag{B9}$$

Inserting $f(t)$ into (B9), and using the fact that for $-\pi\leqslant x\leqslant\pi$ (Gradshteyn and Ryzhik, 1980):

$$\sum_{n=1}^{\infty}(-1)^{n-1}\frac{\cos nx}{n^2}=\frac{\pi^2}{12}-\frac{x^2}{4} \tag{B10}$$

one can obtain readily from (B9) that

(i) for $0 < t \leqslant t_c$,

$$u(z,t)=\frac{qh}{k}\left[\frac{\alpha t}{h^2}+\frac{1}{2}\left(\frac{z^2}{h^2}-\frac{1}{3}\right)-\frac{2}{h^2}\sum_{n=1}^{\infty}\frac{(-1)^n}{\lambda_n^2}e^{-\alpha\lambda_n^2 t}\cos\lambda_n z\right]; \tag{18a}$$

(ii) for $t \geqslant t_c$,

$$u(z,t)=\frac{qh}{k}\left[\frac{\alpha t_c}{h^2}+\frac{2}{h^2}\sum_{n=1}^{\infty}\frac{(-1)^n}{\lambda_n^2}(e^{-\alpha\lambda_n^2(t-t_c)}-e^{-\alpha\lambda_n^2 t})\cos\lambda_n z\right]. \tag{18b}$$